IET Communications

Research Article

Low-complexity PTS schemes using OFDM signal rotation and pre-exclusion of phase rotating vectors

ISSN 1751-8628
Received on 25th February 2015
Revised on 18th October 2015
Accepted on 30th December 2015
doi: 10.1049/iet-com.2015.0192
www.ietdl.org

Kang-Seok Lee[1], *Young-Jeon Cho*[1], *Jun-Young Woo*[1], *Jong-Seon No*[1], *Dong-Joon Shin*[2] ✉

[1]*Department of Electrical and Computer Engineering, INMC, Seoul National University, Seoul 151–744, Korea*
[2]*Department of Electronic Engineering, Hanyang University, Seoul 133–791, Korea*
✉ *E-mail: djshin@hanyang.ac.kr*

Abstract: Partial transmit sequence (PTS), a well-known peak-to-average power ratio (PAPR) reduction scheme for orthogonal frequency division multiplexing (OFDM) systems, has been actively investigated to reduce its high computational complexity. Ku *et al.* proposed a selection method of dominant time-domain samples and by only using the selected samples, the PAPR of each alternative OFDM signal vector is calculated. This method clearly reduces the computational complexity but it is crucial to select proper time-domain samples to achieve acceptable PAPR reduction performance. In this study, a new selection method of dominant time-domain samples is proposed based on rotating samples of inverse fast Fourier transformed (IFFTed) subblocks to the local area on which the corresponding sample of the IFFTed first subblock is located. Moreover, pre-exclusion of phase rotating vectors based on the above time-domain sample rotation is proposed to further reduce the computational complexity. Numerical results confirm that the proposed PTS schemes substantially reduce the computational complexity with negligible degradation of PAPR reduction performance.

1 Introduction

Orthogonal frequency division multiplexing (OFDM) has been widely used in various wireless communication systems such as the wireless local-area network 802.11a/g/n standards, the downlink of the 3GPP long term evolution, and digital video broadcasting due to its bandwidth efficiency and robustness against fading channel. However, OFDM signals show high peak-to-average power ratio (PAPR) which degrades the efficiency of non-linear high power amplifier at the transmitter.

To mitigate this high PAPR problem, various schemes have been proposed such as clipping [1], selected mapping [2], partial transmit sequence (PTS) [3], and tone reservation [4]. Among them, PTS scheme transmits an OFDM signal without signal distortion. However, it has high computational complexity due to the generation of many alternative OFDM signal vectors and hence results in data rate loss due to side information.

The computational complexity of PTS scheme increases exponentially with the number of subblocks because of the PAPR calculation of all alternative OFDM signal vectors. When the number of inverse fast Fourier transforms (IFFTs) is fixed, the computational complexity of PTS scheme is determined by the generation and PAPR calculation of alternative OFDM signal vectors.

To effectively reduce the number of alternative OFDM signal vectors, many low-complexity PTS schemes have been proposed [5–9]. On the other hand, to reduce the computational complexity for calculation and comparison of PAPRs of alternative OFDM signal vectors, a reduced-complexity PTS (RC-PTS) was proposed [10]. In the RC-PTS, sum of the powers of the nth time-domain samples of all inverse fast Fourier transformed (IFFTed) subblocks is calculated for all n to find the dominant time-domain samples by checking if each power sum exceeds the preset threshold. Only the selected dominant time-domain samples are multiplied with the phase rotating vectors for estimaitng the PAPR of each alternative OFDM signal vector, which substantially reduces the computational complexity.

In this paper, a new selection method of dominant time-domain samples in PTS scheme is proposed based on rotating samples of IFFTed subblocks to the local area on which the corresponding sample of the IFFTed first subblock is located. Moreover, pre-exclusion of phase rotating vectors based on the above time-domain sample rotation is proposed to further reduce the computational complexity. Numerical results confirm that the proposed PTS schemes substantially reduce the computational complexity with negligible degradation of PAPR reduction performance.

The rest of the paper is organised as follows. In Section 2, OFDM, PAPR, conventional PTS, and RC-PTS are briefly reviewed. Then, in Section 3, new low-complexity PTS schemes based on time-domain sample rotation and pre-exclusion of the phase rotating vectors are proposed. In Section 4, the computational complexity of the proposed PTS schemes is analysed and the simulation results are provided. Finally, conclusions are given in Section 5.

2 OFDM and PTS

2.1 OFDM and PAPR

In OFDM systems, serial data bits are usually modulated by phase shift keying or quadrature amplitude modulation (QAM). After serial to parallel conversion of N modulated input symbols, an L-times oversampled input symbol vector $\boldsymbol{X}$ of length LN is obtained as $\boldsymbol{X} = [X_0, X_1, \ldots, X_{\mathrm{LN}-1}]^{\mathrm{T}}$, where X_k, $k = 0, 1, \ldots, N-1$, are input symbols and X_k, $k = N, N+1, \ldots, LN-1$, are all zeros padded for L-times oversampling.

By applying IFFT to the input symbol vector $\boldsymbol{X}$, an OFDM signal vector $\boldsymbol{x} = [x_0, x_1, \ldots, x_{\mathrm{LN}-1}]^{\mathrm{T}}$ in the time domain is obtained as

$$x_n = \frac{1}{\sqrt{\mathrm{LN}}} \sum_{k=0}^{N-1} X_k e^{j2\pi kn/LN}, \; 0 \le n \le \mathrm{LN} - 1, \tag{1}$$

where L is the oversampling factor.

The PAPR of the OFDM signal vector $\boldsymbol{x}$ is defined as the ratio of the peak power to the average power of $\boldsymbol{x}$, that is,

$$\mathrm{PAPR}(\boldsymbol{x}) = \frac{\max_{n=0}^{\mathrm{LN}-1} |x_n|^2}{E[|x_n|^2]} \quad (2)$$

where $E[\cdot]$ denotes the expectation.

2.2 Conventional PTS scheme

In the conventional PTS scheme in Fig. 1, an input symbol vector $\boldsymbol{X}$ is partitioned into M disjoint input symbol subblocks $\boldsymbol{X}_m = [X_{m,0}, X_{m,1}, \ldots, X_{m,\mathrm{LN}-1}]^{\mathrm{T}}$, $0 \le m \le M-1$, such that

$$\boldsymbol{X} = \sum_{m=0}^{M-1} \boldsymbol{X}_m \quad (3)$$

where $X_{m,n}$ is either X_n or zero. The input symbol subblocks $\boldsymbol{X}_m$ are transformed into the time-domain signal vectors $\boldsymbol{x}_m = [x_{m,0}, x_{m,1}, \ldots, x_{m,\mathrm{LN}-1}]^{\mathrm{T}}$ by IFFT. Then, the phase rotating factor $b_m^{(u)} = \mathrm{e}^{\mathrm{j}\phi_m^{(u)}}$ with $\phi_m^{(u)} \in [0, 2\pi)$ is multiplied to $\boldsymbol{x}_m$ and the uth alternative OFDM signal vector $\boldsymbol{x}^{(u)}$ is obtained as

$$\boldsymbol{x}^{(u)} = [x_0^{(u)}, x_1^{(u)}, \ldots, x_{\mathrm{LN}-1}^{(u)}]^{\mathrm{T}} = \sum_{m=0}^{M-1} b_m^{(u)} \boldsymbol{x}_m \quad (4)$$

where $u = 0, 1, \ldots, U-1$, and U is the number of total alternative OFDM signal vectors. In general, $b_m^{(u)}$ is an element of the finite set given by

$$b_m^{(u)} \in \{\mathrm{e}^{\mathrm{j}2\pi l/W} | l = 0, 1, \ldots, W-1\} \quad (5)$$

where W is the number of allowed phase rotating factors and the phase rotating vector $\boldsymbol{b}^{(u)}$ to generate the uth alternative OFDM signal vector is defined as $\boldsymbol{b}^{(u)} = [b_0^{(u)}, b_1^{(u)}, \ldots, b_{M-1}^{(u)}]$. Since we can always set $b_0^{(u)} = 1$, we have $U = W^{M-1}$.

Finally, the OFDM signal vector $\boldsymbol{x}^{(u_{\mathrm{opt}})}$ with the minimum PAPR is selected and transmitted, that is,

$$u_{\mathrm{opt}} = \arg\min_{u=0}^{U-1} \mathrm{PAPR}(\boldsymbol{x}^{(u)}) \quad (6)$$

where u_{opt} indicates the optimal phase rotating vector $\boldsymbol{b}^{(u_{\mathrm{opt}})}$ and $\boldsymbol{x}^{(u_{\mathrm{opt}})}$ is transmitted with side information about u_{opt}.

2.3 Reduced-complexity PTS

RC-PTS was proposed to reduce the computational complexity of the conventional PTS scheme [10]. It utilises only a part of time-domain samples to estimate the peak power of each alternative OFDM signal vector, which are selected by using a metric given as [10]

$$Q_n = \sum_{m=0}^{M-1} |x_{m,n}|^2. \quad (7)$$

For each n, if Q_n is greater than or equal to a preset threshold γ, the time-domain samples with the index n in all $\boldsymbol{x}_m$ are called dominant time-domain samples. Denote the set of indices of dominant time-domain samples by

$$\boldsymbol{S}_Q(\gamma) = \{n | Q_n \ge \gamma, \quad 0 \le n \le \mathrm{LN}-1\}. \quad (8)$$

Only the dominant time-domain samples with indices in $S_Q(\gamma)$ are multiplied by the corresponding phase rotating vectors and those values are used to estimate the PAPR of each alternative OFDM signal vector. Then, the OFDM signal vector $\boldsymbol{x}^{(u_{\mathrm{opt}})}$ with the minimum PAPR is selected and transmitted, that is,

$$u_{\mathrm{opt}} = \arg\min_{u=0}^{U-1} \max_{n \in \boldsymbol{S}_Q(\gamma)} \left| \sum_{m=0}^{M-1} b_m^{(u)} x_{m,n} \right|^2. \quad (9)$$

Although the number of alternative OFDM signal vectors of RC-PTS is the same as that of the conventional PTS scheme, it is clear that the computational complexity of RC-PTS is significantly less than that of the conventional PTS scheme.

3 New low-complexity PTS schemes

In this section, two methods for reducing the computational complexity of PTS schemes are proposed. In Section 3.1, new criteria to select dominant time-domain samples are proposed and to further reduce the complexity, pre-exclusion of some phase rotating vectors is proposed in Section 3.2. By combining these methods, three new low-complexity PTS schemes are proposed in Section 3.3.

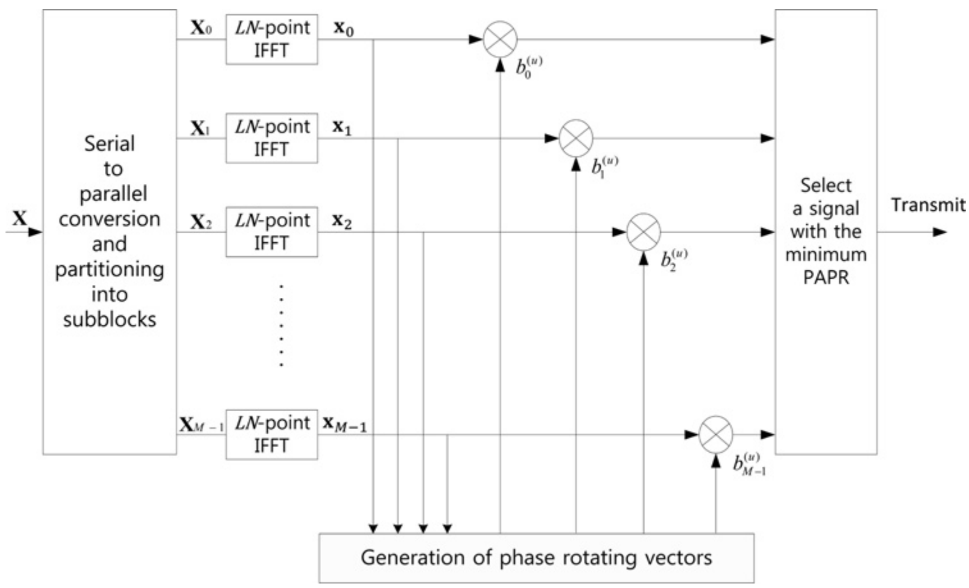

Fig. 1 *Block diagram of the conventional PTS scheme*

3.1 New criteria to select dominant time-domain samples using proper sample rotation

Let V_n denote the maximum power of the nth sample among U alternative OFDM signal vectors in the conventional PTS scheme, which is

$$V_n = \max_{u=0}^{U-1} \left|x_n^{(u)}\right|^2 = \max_{u=0}^{U-1} \left|\sum_{m=0}^{M-1} b_m^{(u)} x_{m,n}\right|^2, \quad n = 0, 1, \ldots, \mathrm{LN}-1 \tag{10}$$

where $b_m^{(u)}$ and the metric V_n constitute the nth phase rotating vector $\boldsymbol{b}^{(u)} = [b_0^{(u)}, b_1^{(u)}, \ldots, b_{M-1}^{(u)}]$ and $\boldsymbol{V} = [V_0, V_1, \ldots, V_{N-1}]$, respectively. In other words, V_n indicates the upper bound of the powers obtained from the nth samples of the alternative OFDM signal vectors. It implies that bigger V_n means higher probability of peak powers of the alternative OFDM signal vectors occurring at the nth sample. Therefore V_n is the proper metric for selecting dominant time-domain samples which practically determine the PAPRs of the alternative OFDM signal vectors.

For a preset threshold γ, the index set of the dominant time-domain samples is obtained as

$$\boldsymbol{S}_V(\gamma) = \{n | V_n \geq \gamma, \quad 0 \leq n \leq \mathrm{LN}-1\}. \tag{11}$$

Instead of using all time-domain samples, by only using the dominant time-domain samples with indices in $\boldsymbol{S}_V(\gamma)$, we calculate the PAPRs of all alternative OFDM signal vectors. However, full search over all phase rotating vectors must be performed to find V_n, which requires $U = W^{M-1}$ searches. Note that if $\gamma = 0$, then this is identical to the conventional PTS scheme.

Thus, in this section, we propose new criteria for estimating V_n with significantly less computational complexity by properly rotating time-domain signal samples without doing full search over all phase rotating vectors. In order to correctly estimate the maximum power V_n of the nth time-domain sample for all alternative OFDM signal vectors, the nth IFFTed signal sample of the mth subblock $x_{m,n}$ is rotated to the sub-plane in the complex plane on which $x_{0,n}$ of the first subblock is located. This will be more clearly explained by using examples as follows.

Fig. 2 shows four different types of rotation of signal samples by 0° or 180° to four sub-planes (shaded areas) containing $x_{0,n}$ in the complex plane for $M = 4$ and $W = 2$. In Fig. 2*a*, the nth IFFTed signal sample of each subblock is rotated to the first and the second quadrants by multiplying proper phase rotating factor in $\{1, -1\}$. In Fig. 2*b*, the nth IFFTed signal sample of each subblock is rotated to the second and the third quadrants by

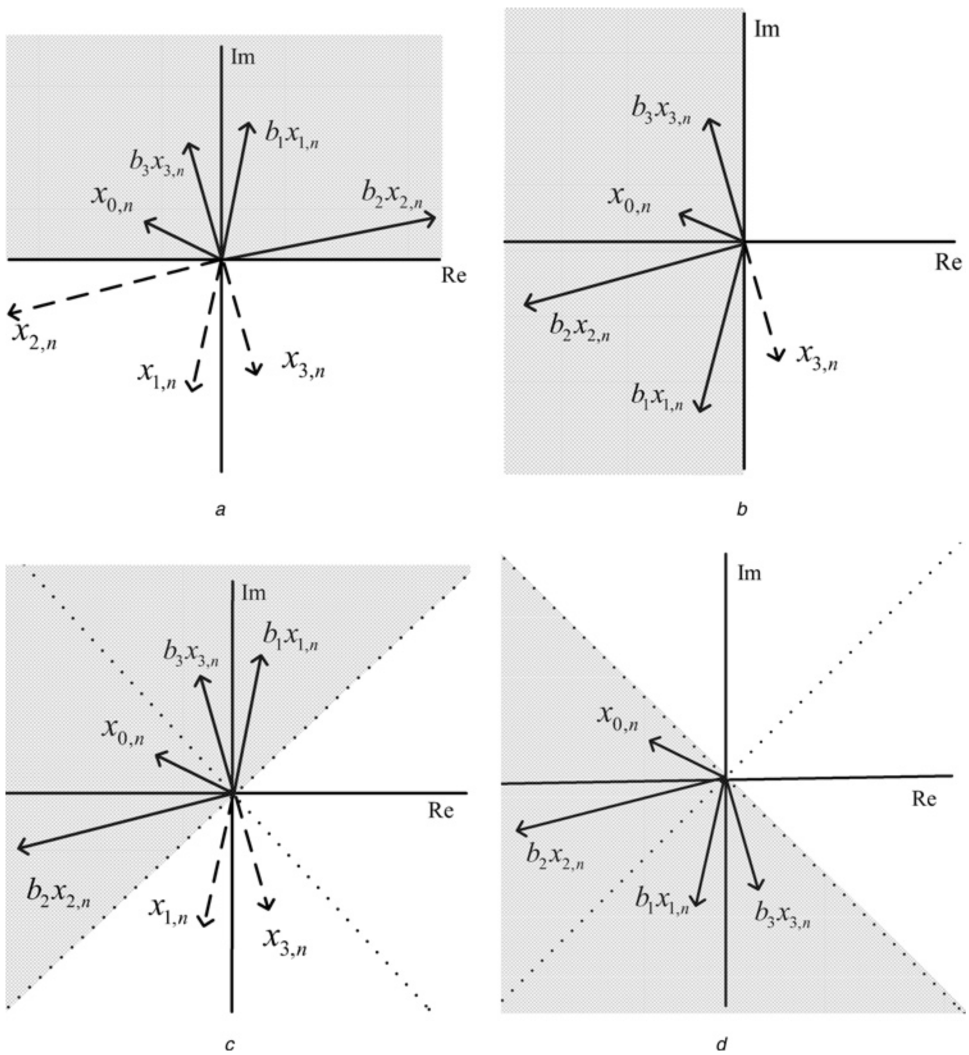

Fig. 2 *Rotation of the nth IFFTed signal samples by 0° or 180° to the shaded sub-plane containing the IFFTed signal sample $x_{0,n}$ of the first subblock using $(1, b_{1,n}, b_{2,n}, b_{3,n})$*

a (1, −1, −1, −1)
b (1, 1, 1, −1)
c (1, −1, 1, −1)
d (1, 1, 1, 1) for $M = 4$ and $W = 2$

multiplying proper phase rotating factor in $\{1, -1\}$. Figs. 2c and 2d show the rotation of the IFFTed signal sample to the sub-planes above 45°−line and below 135°−line, respectively. Note that for binary phase factors 1 and −1, each sub-plane covers 180°−sub-plane because by multiplying −1, the phase is changed by 180°.

In the case of $M = 4$ and $W = 2$, 8 ($= W^{M-1}$) searches are required to find the real maximum power V_n of the nth time-domain sample. However, it is verified through simulation that only four searches given in Fig. 2 are good enough to find the maximum power V_n with high probability. Therefore, by using the proposed criteria to select dominant time-domain samples, the computational complexity for search is remarkably reduced while keeping almost the same search performance as that of the conventional PTS. We can see that by performing four searches given in Fig. 2, the real maximum power is obtained with the probability 0.997. In fact, this result is obtained through extensive simulation which counts how many results obtained by performing searches given in Fig. 2 are matched with the real maximum powers. Note that we may perform any number of searches between 1 and 8 by choosing the same number of 180°-sub-planes and there is a tradeoff between the search performance and the computational complexity.

Fig. 3 shows two different types of rotation of signal samples by 0°, 90°, 180°, or 270° to two sub-planes (shaded areas) containing $x_{0,n}$ in the complex plane by multiplying proper phase rotating factor in $\{1, j, -1, -j\}$ for $M = 4$ and $W = 4$ to estimate V_n. In this case, only two searches are performed among $U = W^{M-1} = 64$ searches to estimate the maximum power V_n of the nth time-domain sample and therefore even more computational complexity reduction is achieved than the case of Fig. 2 with $M = 4$ and $W = 2$. Numerical analysis shows that the real maximum power is obtained with the probability 0.903 by two searches in Fig. 3. Note that for the case of $W = 4$ using quaternary phase factors 1, j, −1, and $-j$, each sub-plane covers 90°−sub-plane and the number of searches can be determined by considering the tradeoff between the search performance and the complexity.

From Figs. 2 and 3, the proposed criteria based on rotating time-domain samples is explained for the cases of $W = 2$ and $W = 4$. Note that the number of searches is determined by considering W, M, and the tradeoff between the search performance and the complexity. In more detail, among total $U = W^{M-1}$ searches, a proper number of 360°/W-sub-planes containing $x_{0,n}$ in the complex plane are selected and the rotation of signal samples to each sub-plane is performed to estimate the maximum power of the nth time-domain sample. Let $\boldsymbol{Z}_U = \{0, 1, \ldots, U-1\}$. By using the criteria in Figs. 2 and 3, we calculate the powers of C ($= 4$ or 2) alternative time-domain samples at the nth sample position after rotating time-domain signal samples, which are denoted as $x_n^{(K_n(0))}, x_n^{(K_n(1))}, \ldots, x_n^{(K_n(C-1))}$, where $K_n(i) \in \boldsymbol{Z}_U$ is the index of the corresponding one among U alternative OFDM signal vectors. Therefore, a new metric P_n to estimate the maximum power V_n is proposed as

$$P_n = \max_{c=0}^{C-1} \left| x_n^{(K_n(c))} \right|^2. \tag{12}$$

Let $\boldsymbol{S}_\mathrm{P}(\gamma_\mathrm{p})$ be the index set of dominant time-domain samples obtained by using P_n such as

$$\boldsymbol{S}_\mathrm{P}(\gamma_\mathrm{p}) = \{n | P_n \geq \gamma_\mathrm{p}, \quad 0 \leq n \leq \mathrm{LN}-1\} \tag{13}$$

where γ_p is a preset threshold. Then only the samples of IFFTed subblocks with the indices in $\boldsymbol{S}_\mathrm{P}(\gamma_\mathrm{p})$ are used for calculating the PAPR of each alternative OFDM signal vector. If P_n is a good approximation of V_n, a substantial reduction of computational complexity can be achieved.

Now, we evaluate the estimation error of V_n by using P_n through the normalised mean square error (NMSE) defined by

$$\mathrm{NMSE}(P_n) = \frac{1}{\mathrm{LN}} \sum_{n=0}^{\mathrm{LN}-1} \frac{(P_n - V_n)^2}{E[P_n]E[V_n]}. \tag{14}$$

Table 1 compares the NMSE for the cases of using P_n or Q_n when $C = 4$ (for $W = 2$) or 2 (for $W = 4$), $L = 4$, and $N = 1024$ for various number of subblocks M. The NMSE for the P_n case is much lower than that of the Q_n case regardless of M, which means that P_n approximates V_n more closely than Q_n does.

The generalised procedures of the proposed selection criteria for selecting dominant time-domain samples for arbitrary M and W are summarised as follows:

(a) Candidate sub-planes which can be used for the proposed selection criteria are all the 360°/W-sub-planes containing $x_{0,n}$ in the complex plane, $0 \leq n \leq \mathrm{LN}-1$.
(b) Among candidate sub-planes, select C sub-planes for the proposed selection criteria such that the boundaries of sub-planes are located as far as possible in terms of relative angle.
(c) By using the selected C sub-planes, find the set $\{K_n(0), K_n(1), \ldots, K_n(C-1)\}$ and calculate P_n by using (12).
(d) Construct $\boldsymbol{S}_\mathrm{P}(\gamma_\mathrm{p})$ by using (13).

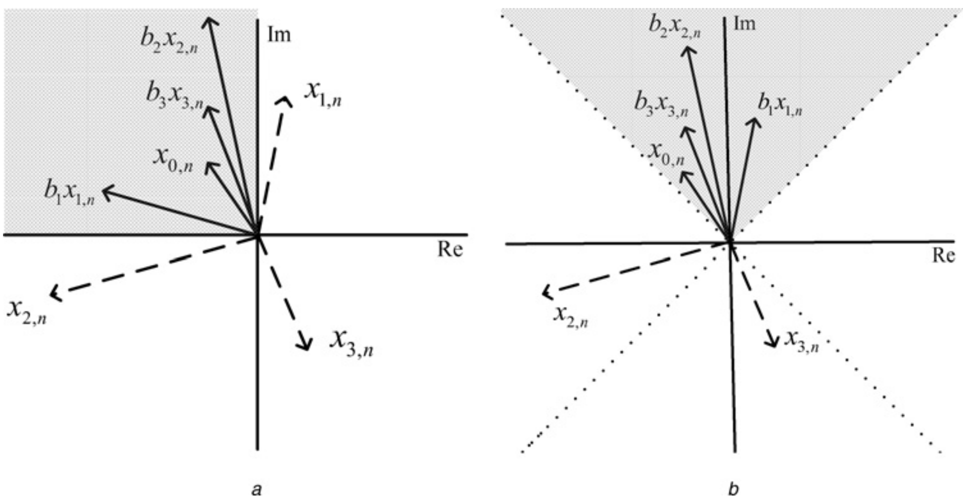

Fig. 3 *Rotation of the nth IFFTed signal samples by 0°, 90°, 180°, or 270° to the shaded sub-plane containing the IFFTed signal sample $x_{0,n}$ of the first subblock using (1, $b_{1,n}$, $b_{2,n}$, $b_{3,n}$)*
a (1, j, $-j$, −1)
b (1, 1, $-j$, −1) for $M = 4$ and $W = 4$

Table 1 NMSE for estimating V_n by using P_n or Q_n when $L=4$ and $N=1024$

Number of subblocks, M	$W=2$ and $C=4$		$W=4$ and $C=2$	
	P_n	Q_n	P_n	Q_n
4	1.4×10^{-5}	5.4×10^{-3}	1.0×10^{-4}	6.7×10^{-3}
6	4.0×10^{-5}	6.9×10^{-3}	1.4×10^{-4}	8.2×10^{-3}
8	6.6×10^{-5}	7.8×10^{-3}	1.6×10^{-4}	9.1×10^{-3}

Note that the number of subblocks M clearly affects the number of sub-planes C used for the proposed selection criteria. As M increases, C also increases to keep the search performance. C should be determined by considering the tradeoff between the estimation performance and the computational complexity mostly through simulation.

3.2 Pre-exclusion of phase rotating vectors

The complexity of the proposed low-complexity scheme in Section 3.1 can be further reduced by excluding some phase rotating vectors which give large sample powers before calculating the PAPR, which is called pre-exclusion of phase rotating vectors. Let $\boldsymbol{E}_\mathrm{P}$ be the set of indices of phase rotating vectors which give large sample powers defined by

$$\boldsymbol{E}_\mathrm{P}=\left\{K_n(i)\,\middle|\,\left|x_n^{(K_n(c))}\right|^2\ge\gamma_v,\quad 0\le c\le C-1,\quad 0\le n\le \mathrm{LN}-1\right\} \tag{15}$$

where γ_v is a preset threshold to find the phase rotating vectors which are excluded from U phase rotating vectors before calculating PAPR of each alternative OFDM signal vector. Therefore, we use the phase rotating vectors with the indices in $\boldsymbol{E}_S=\boldsymbol{Z}_U-\boldsymbol{E}_\mathrm{P}$ to generate alternative OFDM signal vectors instead of using all U phase rotating vectors. The total number of phase rotating vectors used for PAPR calculation is $|\boldsymbol{E}_S|$.

3.3 Low-complexity PTS schemes

By combining the proposed methods in Sections 3.1 and 3.2, the optimal phase rotating vector $\boldsymbol{b}^{(u_\mathrm{opt})}$ is obtained as

$$u_\mathrm{opt}=\arg\min_{u\in\boldsymbol{E}_S}\frac{\max_{n\in\boldsymbol{S}_\mathrm{P}(\gamma_\mathrm{p})}\left|\sum_{m=0}^{M-1}b_m^{(u)}x_{m,n}\right|^2}{E[|x_n|^2]}, \tag{16}$$

which is based on the selection of dominant time-domain samples by using P_n and the pre-exclusion of phase rotating vectors. Fig. 4 shows a block diagram of the proposed PTS scheme to find $\boldsymbol{x}^{(u_\mathrm{opt})}$ by using (16).

Now, we propose three low-complexity PTS schemes utilising the results in the previous sections, that is, a PTS scheme using dominant time-domain samples selected by P_n (PS-PTS), a PTS scheme by excluding phase rotating vectors using all time-domain samples (PE-PTS), and a PTS scheme combining dominant time-domain samples selected by P_n and pre-exclusion (PC-PTS) which is equivalent to (16).

The detailed procedures of three proposed low-complexity PTS schemes are summarised as follows:

(i) PS-PTS scheme
(a) An input data vector is partitioned into M disjoint subblocks and each of them is IFFTed.
(b) Select sub-planes in the complex plane to which the time-domain signal samples are rotated and calculate P_n in (10) at each sample position n.
(c) Find the index set $\boldsymbol{S}_\mathrm{P}(\gamma_\mathrm{p})$ by using a proper threshold γ_p.
(d) Only the dominant time-domain samples with the indices in $\boldsymbol{S}_\mathrm{P}(\gamma_\mathrm{p})$ are used to calculate the PAPRs of alternative OFDM signal vectors and the optimal phase rotating vector $\boldsymbol{b}^{(u_\mathrm{opt})}$ is selected.
(e) Generate $\boldsymbol{x}^{(u_\mathrm{opt})}$ by using $\boldsymbol{b}^{(u_\mathrm{opt})}$ and transmit it.

(ii) PE-PTS scheme
(a) An input data vector is partitioned into M disjoint subblocks and each of them is IFFTed.
(b) Select sub-planes in the complex plane to which the time-domain signal samples are rotated and find pre-excluded phase rotating vectors using (15).
(c) Only the survived phase rotating vectors are used to generate alternative OFDM signal vectors and calculate the PAPRs of them, and the optimal phase rotating vector $\boldsymbol{b}^{(u_\mathrm{opt})}$ is selected.
(d) Generate $\boldsymbol{x}^{(u_\mathrm{opt})}$ by using $\boldsymbol{b}^{(u_\mathrm{opt})}$ and transmit it.

(iii) PC-PTS scheme
(a) An input data vector is partitioned into M disjoint subblocks and each of them is IFFTed.
(b) Select sub-planes in the complex plane to which the time-domain signal samples are rotated.
b-1) Calculate P_n for each n and find the index set $\boldsymbol{S}_\mathrm{P}(\gamma_\mathrm{p})$ with proper γ_p.
b-2) Find the set of indices of pre-excluded phase rotating vectors using (15) and $\boldsymbol{S}_\mathrm{P}(\gamma_\mathrm{p})$.

(c) Only the dominant time-domain samples with the indices in $\boldsymbol{S}_\mathrm{P}(\gamma_\mathrm{p})$ and the survived phase rotating vectors are used to

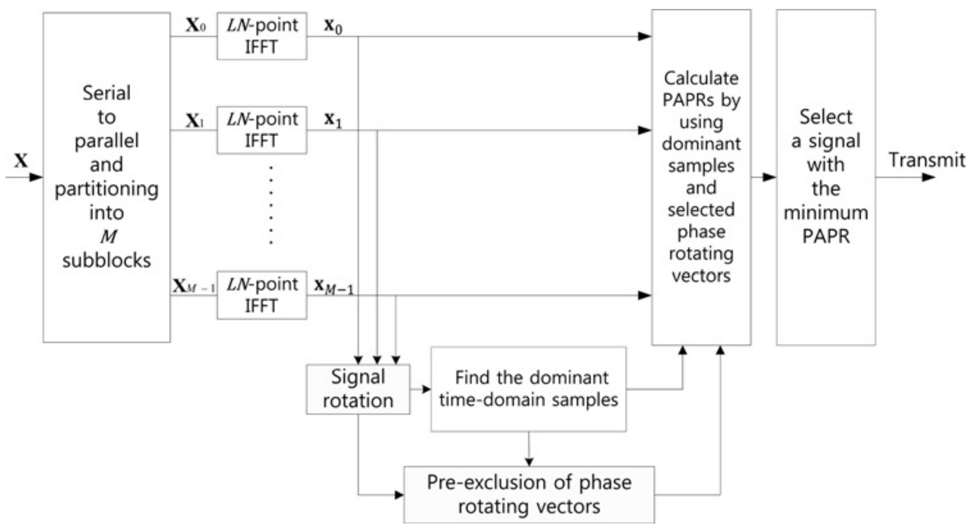

Fig. 4 *Block diagram of the proposed PTS scheme based on signal rotation and pre-exclusion*

IET Commun., 2016, Vol. 10, Iss. 5, pp. 540–547

calculate the PAPRs of alternative OFDM signal vectors and the optimal phase rotating vector $\boldsymbol{b}^{(u_{\text{opt}})}$ is selected.

(d) Generate $\boldsymbol{x}^{(u_{\text{opt}})}$ by using $\boldsymbol{b}^{(u_{\text{opt}})}$ and transmit it.

4 Computational complexity and simulation results

4.1 Computational complexity

In this section, we compare the computational complexity of the conventional PTS, RC-PTS, and the three proposed low-complexity PTS schemes PS-PTS, PE-PTS, and PC-PTS for $M = 8$, $L = 4$, $W = 2$, $N = 1024$, and $C = 4$ as given in Fig. 2. Since the computational complexity in terms of complex addition shows a similar tendency as that in terms of complex multiplication, only the complex multiplications required for generating necessary alternative OFDM signal vectors are considered.

Let N_α denote the number of selected time-domain samples $|S_V(\alpha)|$ for PS-PTS and $|S_Q(\alpha)|$ for PC-PTS. Then, the ratio p_α between the number of selected time-domain samples and the number of all time-domain samples is defined as

$$p_\alpha = \frac{N_\alpha}{\text{LN}}. \tag{17}$$

For fair comparison, through simulation, p_α is set to 0.07 for PS-PTS, PC-PTS and RC-PTS. Note that when p_α is set to 0.07, PS-PTS achieves the same PAPR reduction performance at *CCDF* $= 10^{-4}$ as the conventional PTS. In addition, $|\boldsymbol{E}_s|$ is set to 17 for PE-PTS and PC-PTS in order to achieve the same PAPR reduction performance at *CCDF* $= 10^{-4}$ as the conventional PTS and PS-PTS.

Note that while RC-PTS requires *MLN* complex multiplications to calculate total *LN* metric values Q_n [10], the three proposed low-complexity PTS schemes require *CLN* complex multiplications to calculate *C* power values at *LN* positions. Table 2 shows that compared with the conventional PTS, PC-PTS requires the lowest computational complexity (1.1%) with achieving the same PAPR 8.4 dB at *CCDF* $= 10^{-4}$, whereas the RC-PTS requires the computational complexity (13.3%) with the PAPR 10 dB at CCDF $= 10^{-4}$. Note that the pre-exclusion of phase rotating vectors can be easily combined with the conventional PTS as well as other low-complexity PTS schemes using dominant time-domain samples [11] including RC-PTS.

The PTS schemes proposed in [12] are also low-complexity schemes which is able to achieve the same PAPR reduction performance as the original PTS. In comparison with the PTS with recursive phase weighting in [12], the proposed PTS schemes have much lower computational complexity. Note that whereas the PTS with recursive phase weighting in [12] constantly requires 25% complex multiplications of the conventional PTS to achieve the same PAPR reduction performance as the conventional PTS, the proposed PTS schemes require much smaller number of complex multiplications as given in Table 2.

However, it is difficult to compare the proposed PTS schemes with the PTS with grouping phase weighting in [12] in terms of computational complexity because the computational complexity of each schemes is calculated using different kind of parameters. In detail, although the PTS with grouping phase weighting in [12] require much lower computational complexity to achieve the same PAPR reduction performance as the conventional PTS, corresponding parameters r_i and R which are used only in that scheme and dominantly affect the computational complexity are not specified in the paper. In the case of $M = 4$, the PTS with grouping phase weighting with $r_1 = 2$ and $R = 2$ is provided in [12] and it can be compared with the proposed PTS shcemes in terms of the computational complexity. It is shown in [12] that for $M = 4$, $r_1 = 2$ and $R = 2$, the PTS with grouping phase weighting requires 41.7 and 18.7% complex multiplications of the conventional PTS to achieve the same PAPR reduction performance as the conventional PTS for $W = 2$ and 4, respectively. In the same condition $M = 4$, the proposed PTS schemes require smaller number of complex multiplication to achieve the same PAPR reduction performance as the conventional PTS.

Table 2 Comparison of computational complexity of the conventional PTS, RC-PTS, and the three proposed low-complexity PTS schemes for $M = 8$, $L = 4$, $W = 2$, $N = 1024$, $C = 4$, $p_\alpha = 0.07$ and $|\boldsymbol{E}_s| = 17$

PTS scheme	Number of complex multiplications	PAPR for CCDF = 10^{-4}, dB
conventional	LNU = 524288 (100%)	8.4
RC-PTS	MLN + p_αLNU = 69468 (13.3%)	10
PS-PTS	CLN + p_αLNU = 53084 (10.1%)	8.4
PE-PTS	CLN + LN$|\boldsymbol{E}_s|$ = 86016 (16.4%)	8.4
PC-PTS	CLN + p_αLN$|\boldsymbol{E}_s|$ = 6021 (1.1%)	8.4

4.2 Simulation results

Fig. 5 compares the PAPR reduction performance of the conventional PTS, RC-PTS, and PS-PTS using the criteria in Fig. 3. For simulation, $L = 4$, $M = 4$, $C = 2$, $W = 4$, and 16-QAM are used. The value of p_α is set to 0.01 or 0.03 when $N = 1024$ in Fig. 5*a* and 0.13 or 0.17 when $N = 128$ in Fig. 5*b*, respectively. Note that p_α changes according to γ_p. Fig. 5*a* shows that when $N = 1024$, 3% of time-domain samples are sufficient for PS-PTS to achieve the same PAPR reduction performance as the conventional PTS, whereas by using 3% of time-domain samples, the PAPR reduction performance of RC-PTS degrades by 0.4 dB. Fig. 5*b* shows that when $N = 128$, 13% of time-domain samples are sufficient for PS-PTS to achieve the same PAPR reduction

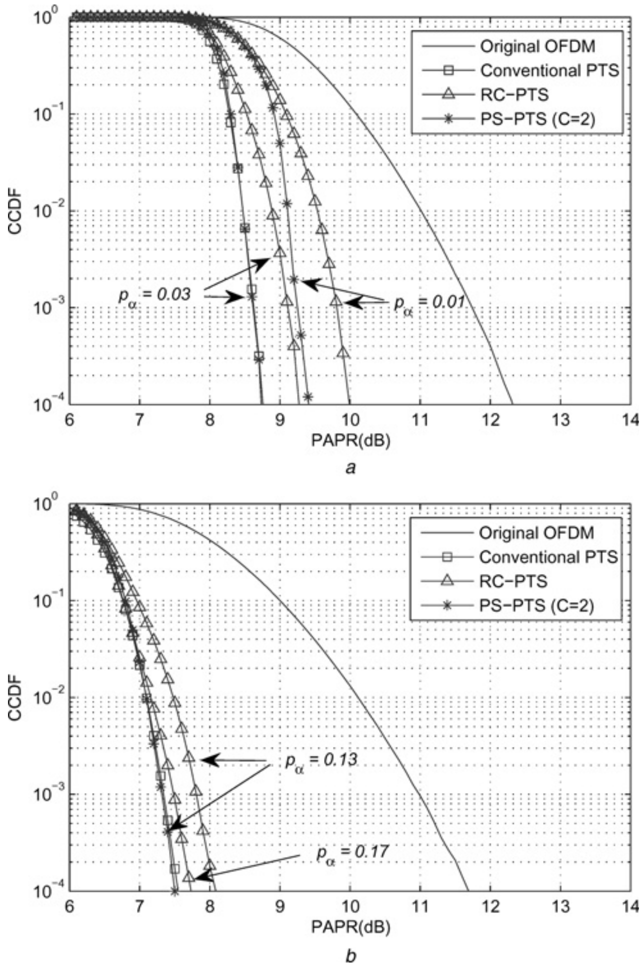

Fig. 5 *Comparison of PAPR reduction performance of the conventional PTS, RC-PTS, and PS-PTS when L = 4, M = 4, C = 2, W = 4 and 16-QAM*

a $N = 1024$ and $p_\alpha = 0.01, 0.03$
b $N = 128$ and $p_\alpha = 0.13, 0.17$

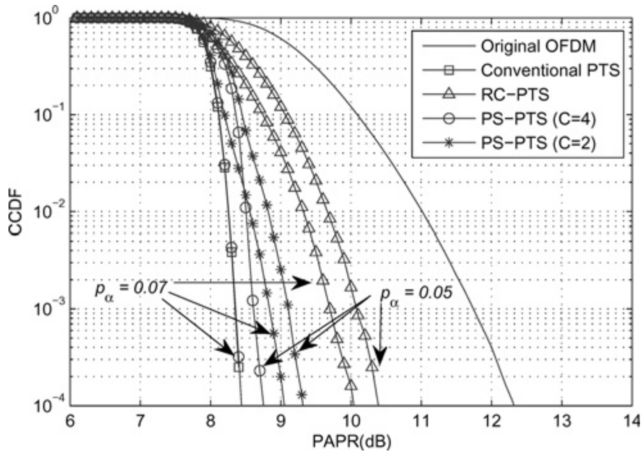

Fig. 6 *Comparison of PAPR reduction performance of the conventional PTS, RC-PTS, and PS-PTS for various C when N = 1024, L = 4, M = 8, W = 2, 16-QAM, and* $p_\alpha = 0.05, 0.07$

performance as the conventional PTS, whereas by using 13% of time-domain samples, the PAPR reduction performance of RC-PTS degrades by 0.6 dB.

Fig. 6 compares the PAPR reduction performance of the conventional PTS, RC-PTS, and PS-PTS for $C = 2$ or 4 when $N = 1024$, $L = 4$, $M = 8$, $W = 2$, 16-QAM, and $p_\alpha = 0.05$, 0.07. Two PS-PTS schemes are simulated such that one is with $C = 2$ of using Figs. 2*a* and *b*, and the other one is with $C = 4$ of using all four cases in Fig. 2. By only using 7% of time-domain samples, PS-PTS with $C = 4$ shows the same PAPR reduction performance as the conventional PTS. Moreover, the PAPR reduction performance of two PS-PTS schemes is better than that of RC-PTS.

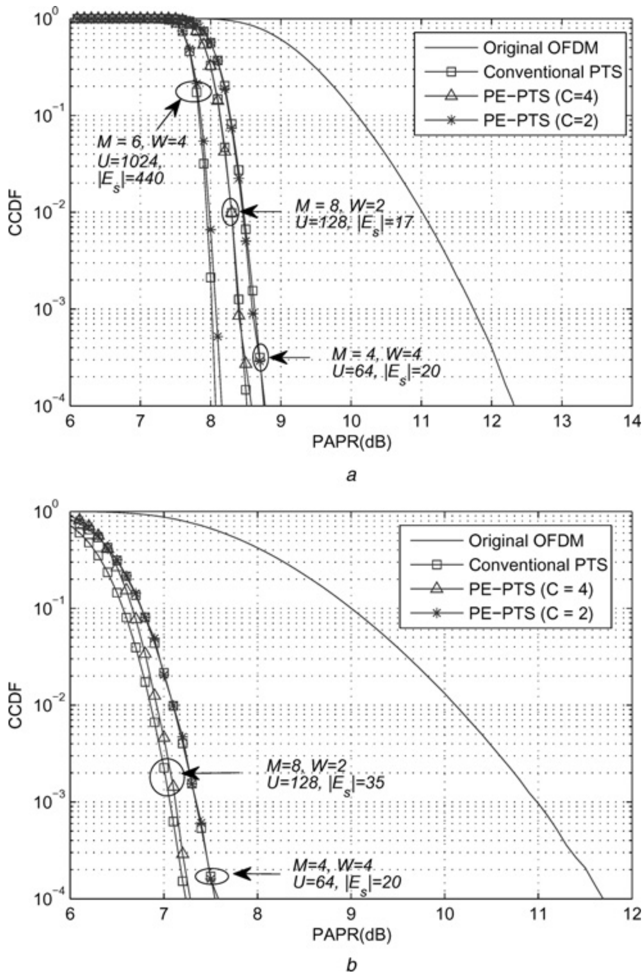

Fig. 7 *Comparison of PAPR reduction performance of the conventional PTS and PE-PTS when*

a $N = 1024$, $L = 4$, 16-QAM, $M = 4, 6, 8$, and $W = 2, 4$
b $N = 128$, $L = 4$, 16-QAM, $M = 4, 8$, and $W = 2, 4$

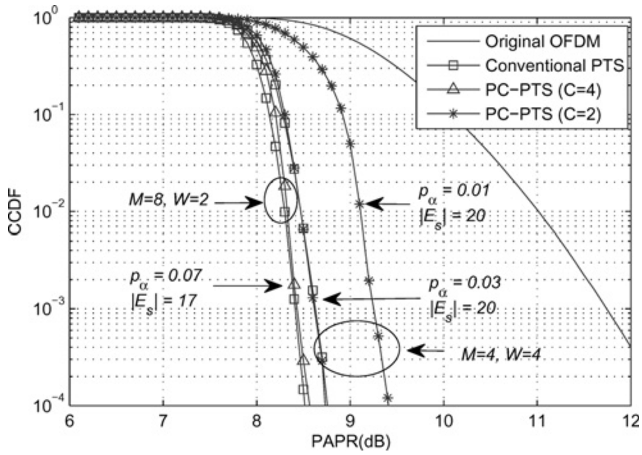

Fig. 8 *Comparison of PAPR reduction performance of the conventional PTS and two PC-PTS schemes when N = 1024, L = 4, 16-QAM, M = 4, 8, and W = 2, 4*

Fig. 7 demonstrates the PAPR reduction performance of the conventional PTS and PE-PTS for the cases of *(a)* $N = 1024$, $L = 4$, 16-QAM, $M = 4$, 6, 8, and $W = 2$, 4 and *(b)* $N = 128$, $L = 4$, 16-QAM, $M = 4$, 8, and $W = 2$, 4. Fig. 7*a* shows that for $M = 8$ and $W = 2$, by using only 17 alternative OFDM signal vectors, PE-PTS achieves the same PAPR reduction performance as the conventional PTS using $U = 128$ alternative OFDM signal vectors. Moreover, to achieve the same PAPR reduction performance as the conventional PTS using $U = 64$ for $M = 4$ and $W = 4$, and $U = 1024$ for $M = 6$ and $W = 4$, PE-PTS needs only $|\boldsymbol{E}_s| = 20$ and 440, respectively. Similarly, it is shown in Fig. 7*b* that PE-PTS requires much smaller number of alternative OFDM signal vectors to achieve almost the same PAPR reduction performance compared with the conventional PTS.

Fig. 8 shows the PAPR reduction performance of PC-PTS for $N = 1024$, $L = 4$, 16-QAM, $M = 4$, 8, and $W = 2$, 4. For $M = 8$ and $W = 2$, by using 17 alternative OFDM signal vectors with $p_\alpha = 0.07$, PC-PTS achieves almost the same PAPR reduction performance as that of the conventional PTS and also substantially reduces the computational complexity to 1.1% compared with the conventional PTS. For $M = 4$ and $W = 4$, it is shown that the PAPR reduction performance of PC-PTS using substantially reduced 20 alternative OFDM signal vectors is almost the same as that of the conventional PTS using 64 alternative OFDM signal vectors.

5 Conclusions

In this paper, three low-complexity PTS schemes are proposed, which substantially reduce the computational complexity. The computational complexity for calculating PAPRs of alternative OFDM signal vectors is reduced by selecting dominant time-domain samples using a new simple metric based on OFDM signal sample rotation. Moreover, the number of considered alternative OFDM signal vectors is reduced by pre-excluding some phase rotating vectors. Numerical analysis shows that the proposed low-complexity PTS schemes can achieve almost the same PAPR reduction performance as that of the conventional PTS scheme with very large computational complexity reduction and also outperforms RC-PTS.

6 References

1 Gross, R., Veeneman, D.: 'Clipping distortion in DMT ADSL systems', *Electron. Lett.*, 1993, **29**, (24), pp. 2080–2081

2 Baüml, R.W., Fischer, R.F.H., Huber, J.B.: 'Reducing the peak-to-average power ratio of multicarrier modulation by selected mapping', *Electron. Lett.*, 1996, **32**, (22), pp. 2056–2057
3 Müller, S.H., Huber, J.B.: 'OFDM with reduced peak-to-average power ratio by optimum combination of partial transmit sequences', *Electron. Lett.*, 1997, **33**, (5), pp. 368–369
4 Tellado, J., Cioffi, J.M.: 'Multicarrier modulation with low PAR: Applications to DSL and wireless' (Norwell, 2000)
5 Lim, D.-W., Heo, S.-J., No, J.-S., *et al.*: 'A new PTS OFDM scheme with low complexity for PAPR reduction', *IEEE Trans. Broadcast.*, 2006, **52**, (1), pp. 77–82
6 Alavi, A., Tellambura, C., Fair, I.: 'PAPR reduction of OFDM signals using partial transmit sequence: an optimal approach using sphere decoding', *IEEE Commun. Lett.*, 2005, **9**, (11), pp. 982–984
7 Wang, Y., Chen, W., Tellambura, C.: 'A PAPR reduction method based on artificial bee colony algorithm for OFDM signals', *IEEE Trans. Wirel. Commun.*, 2010, **9**, (10), pp. 2994–2999
8 Cimini, L.J., Sollenberger, N.R.: 'Peak-to-average power ratio reduction of an OFDM signal using partial transmit sequences', *IEEE Commun. Lett.*, 2000, **4**, (3), pp. 86–88
9 Cho, Y.-J., No, J.-S., Shin, D.-J.: 'A new low-complexity PTS scheme based on successive local search using sequences', *IEEE Commun. Lett.*, 2012, **16**, (9), pp. 1470–1473
10 Ku, S.-J., Wang, C.-L., Chen, C.-H.: 'A reduced-complexity PTS-based PAPR reduction scheme for OFDM systems', *IEEE Trans. Wirel. Commun.*, 2010, **9**, (8), pp. 2455–2460
11 Xiao, Y., Lei, X., Wen, Q., *et al.*: 'A class of low complexity PTS techniques for PAPR reduction in OFDM systems', *IEEE Signal Process. Lett.*, 2007, **14**, (10), pp. 680–683
12 Wang, L., Liu, J.: 'PAPR reduction of OFDM signals by PTS with grouping and recursive phase weighting methods', *IEEE Trans. Broadcast.*, 2011, **57**, (2), pp. 299–306